

## Supporting Information

### **Epitaxial Transformations of Metal-organic Frameworks into Orientated Superparticles**

Lei Shao,<sup>a</sup> Fanbao Meng,<sup>\*a</sup> Yu Fu,<sup>\*a</sup> and Junyi Chen<sup>\*b</sup>

<sup>a</sup> Department of Chemistry, College of Sciences, Northeastern University, Shenyang 110819, PR China  
E-mail: mengfb@mail.neu.edu.cn; fuyu@mail.neu.edu.cn

<sup>b</sup> Engineering Laboratory of Chemical Resources Utilization in South Xinjiang of Xinjiang Production and Construction Corps, College of Life Science, Tarim University, Xinjiang Uygur Autonomous Region, Alaer 843300, PR China  
Email: sln5xn@163.com

## **Materials**

2,5-dihydroxyterephthalic acid (H<sub>4</sub>DOBDC), copper (II) acetate (Cu(OAc)<sub>2</sub>), N, N-dimethylformamide (DMF), acetonitrile (CH<sub>3</sub>CN), methanol (CH<sub>3</sub>OH), were purchased from Sinopharm Chemical Reagent Co., Ltd. Pure water was purchased from Shenyang Wahaha Group Co., Ltd. All chemicals used in this work were analytical grade and without further purification.

## **Observation and Characterization of Transformation Process**

According to different soaking time, a part of the Crystal PMC was taken out and dried for various morphology and structure characterizations. And the transformation process was detected by monitoring the change in absorbance caused by the dissolution of the excess ligands in the solution.

## **Synthesis of Small Size Pristine MOF Crystal**

A solution of H<sub>4</sub>DOBDC in a mixture of DMF and acetonitrile (3:1 in volume, 5 mL, 30 mmol L<sup>-1</sup>) was mixed with water (0.8 mL) in a glass culture dish. A solution of Cu(OAc)<sub>2</sub> in a mixture of DMF and acetonitrile (3:1 in volume, 1 mL, 70 mmol L<sup>-1</sup>) was added additional 0.4 mL water, and it was added into the H<sub>4</sub>DOBDC solution in a dropwise manner with a rate of 10 μL s<sup>-1</sup> under shaken. Then the solution was stirred for ten minutes and evaporated under the atmosphere with about 60% humidity for 72 h, the pristine MOF crystal was obtained as powder-like crystalline product after filtration and washed with DMF.

## **Energy calculation**

The electronic structures were computed by Vienna ab initio Simulation package (VASP) of density functional theory (DFT). The projector augmented wave (PAW) model with Perdew-Burke-Ernzerhof (PBE) function was employed to describe the interactions between core and electrons, an energy cutoff of 450 eV was used for the planewave expansion of the electronic wave function. The Brillouin zones of all

systems were sampled with gamma-point centered Monkhorst-Pack grids. A  $1 \times 1 \times 4$  Monkhorst Pack k-point setup were used for geometry optimization. The force and energy convergence criterion were set to  $0.02 \text{ eV } \text{\AA}^{-1}$  and  $10^{-5} \text{ eV}$ , respectively. The binding energy is calculated by:

$$E_{coh} = \frac{E_{tot} - N_A E_{atom}^A - N_B E_{atom}^B - N_C E_{atom}^C}{N_A + N_B + N_C} \quad (1)$$

### Calculation of ligand dissolution equilibrium process

4 mg obtained PMC crystals were soaked in 40 ml methanol solution, respectively. Then, the absorbance curves of methanol solutions in different time were monitored with an optics spectrometer every 12 h. The whole dissolution process of the organic ligands from pristine crystals into solution can be described by the time (t) and dissolution extent ( $\alpha$ ) from the absorbance curves (Fig. S11). And the dissolution extent  $\alpha$  can be obtained by following equations:

$$\alpha_t = \frac{A_0 - A_t}{A_0 - A_f} \quad (2)$$

Where  $\alpha$  is always between 0 and 1;  $A_t$  represents the absorbance at the peak of  $\sim 370$  nm in the curve of the solution at arbitrary time t; whereas  $A_0$  and  $A_f$  are the absorbances at the peak of  $\sim 370$  nm in the curve of the solution at the beginning and at the end of the process, respectively.

### Kinetic fitting

The appropriate kinetic model equation is identified by verifying the linearity of plots of calculated values of  $g(\alpha)$  against time:

$$g(\alpha) = kt \quad (3)$$

The common kinetic model expression of integral function  $g(\alpha)$  is proposed from literatures in Table S3

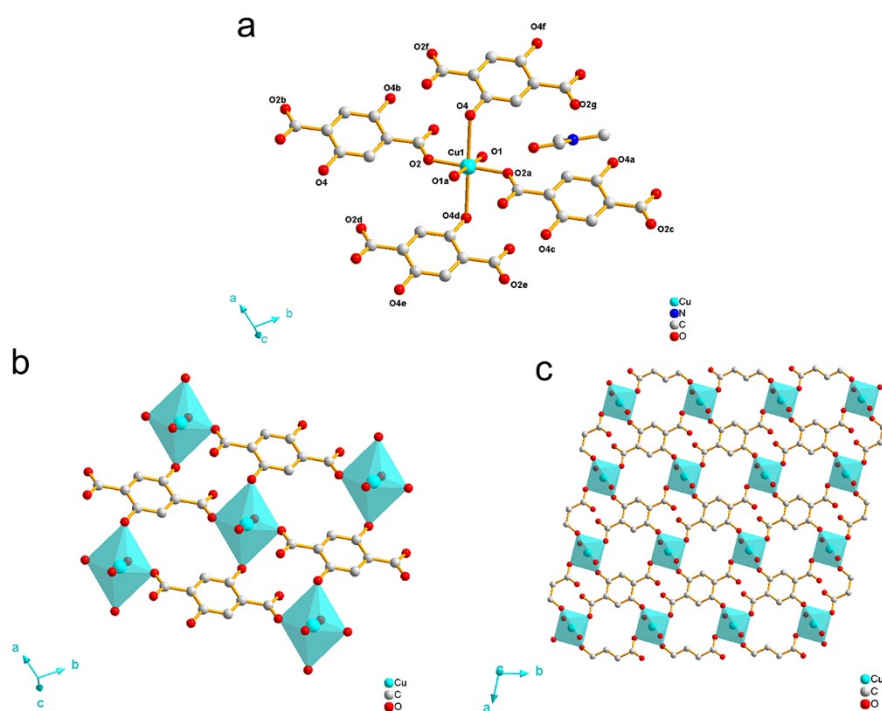


**Fig. S1** Crystal structure of PMC. (a) The fundamental unit of PMC. (b) The coordination environment of  $\text{Cu}^{2+}$  in PMC. (c) The 2D layer structure of PMC. The hydrogen atoms and DMF molecules are omitted for clarity. Symmetry codes: a)  $1-x, 1-y, -z$ ; b)  $2-x, -y, 1-z$ ; c)  $-1+x, 1+y, -z$ ; d)  $1-x, -y, 1-z$ ; e)  $1-x, -y, 1-z$ ; f)  $-1+x, y, z$ ; g)  $2-x, 1-y, 1-z$ .

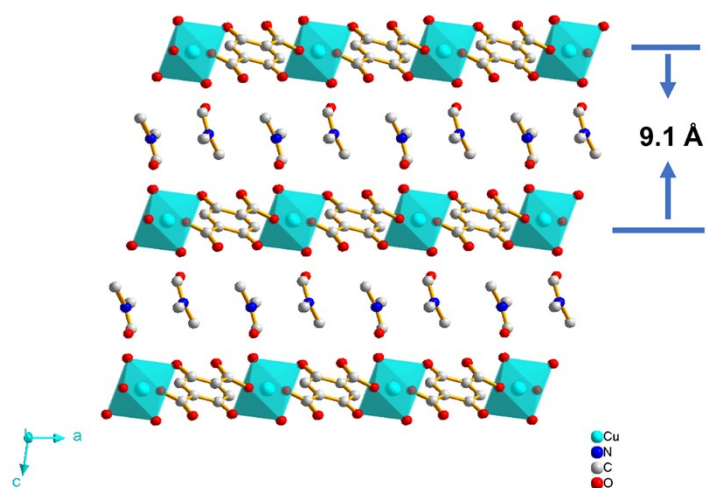


**Fig. S2** The stacked 2D-layer structures with solvent molecules (DMF) in PMC.

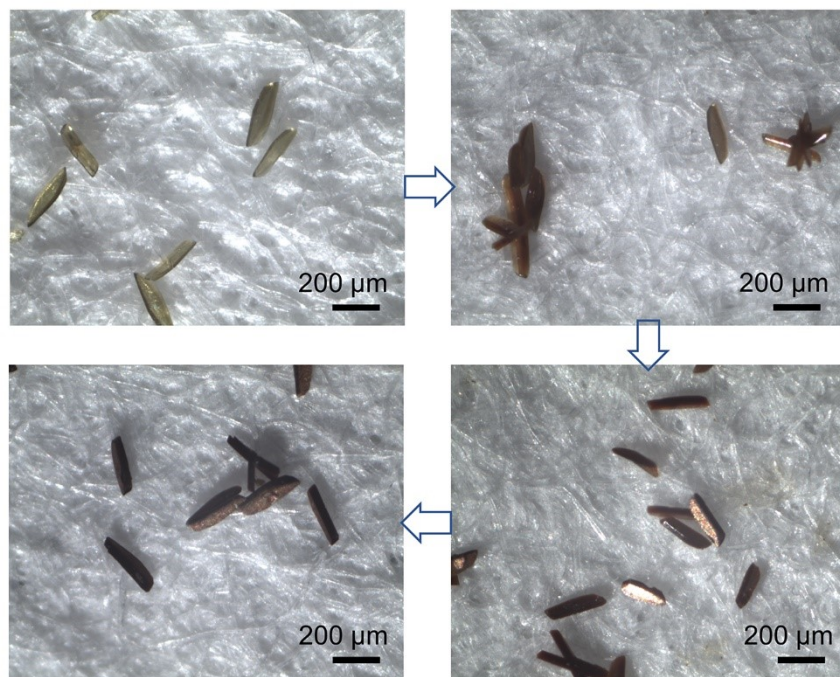


**Fig. S3** The optical photographs for the color and transparency before and after the transformation from PMC to OMS.

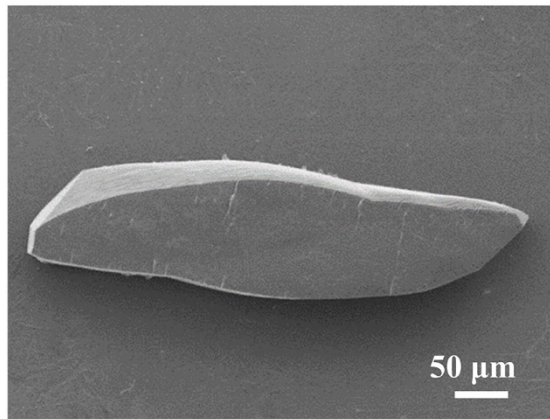


**Fig. S4** SEM images of the PMC.

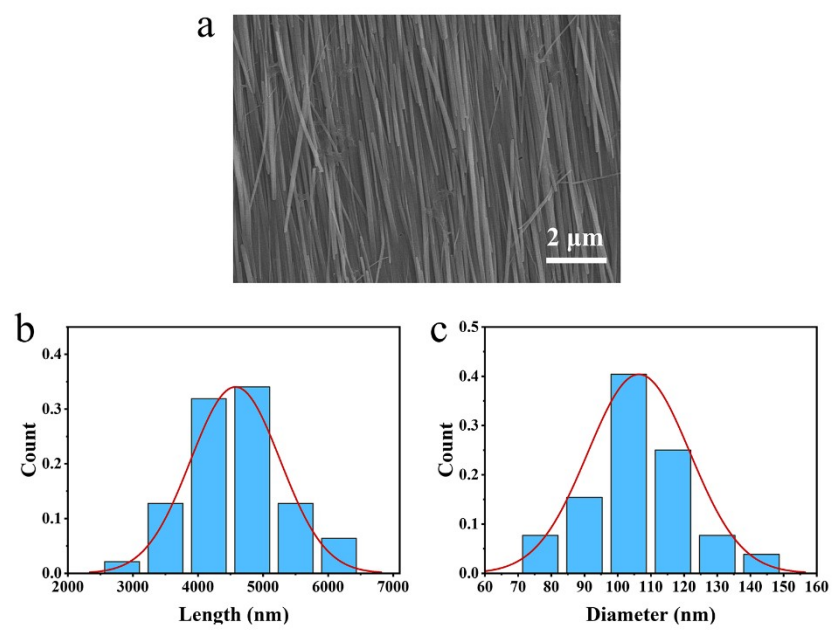


**Fig. S5** The diameter and length distribution of the MOF-74 nanoneedles in the OMS.



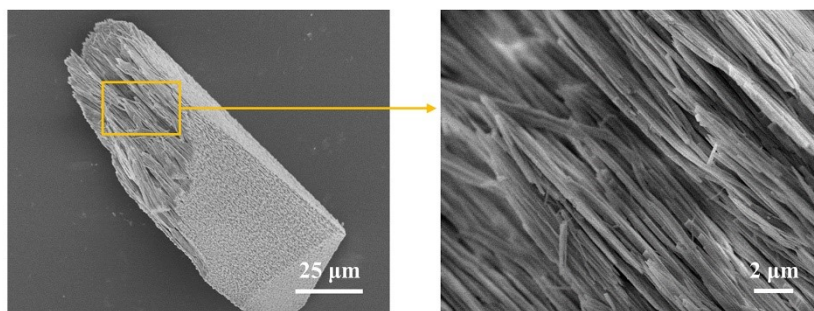


**Fig. S6** The SEM image of internal structure of the cracked OMS.

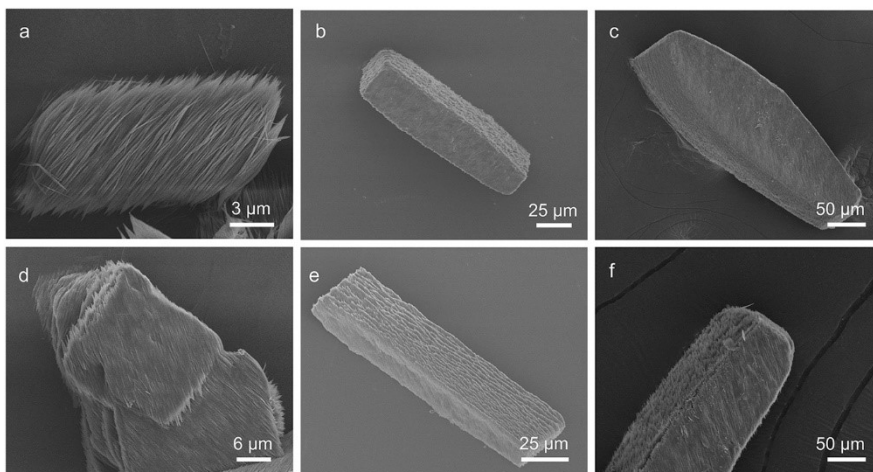


**Fig. S7** The SEM images of obtained OMS samples with different size and morphology.

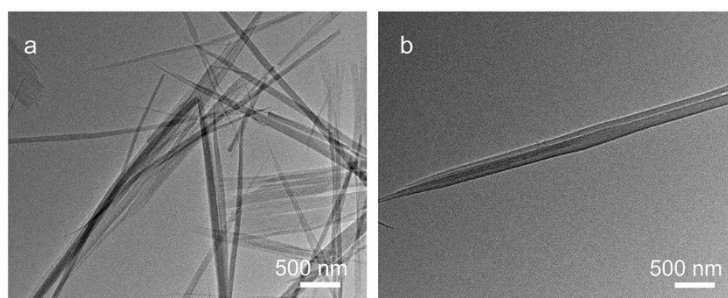


**Fig. S8** The TEM images of separate MOF-74 nanoneedles.

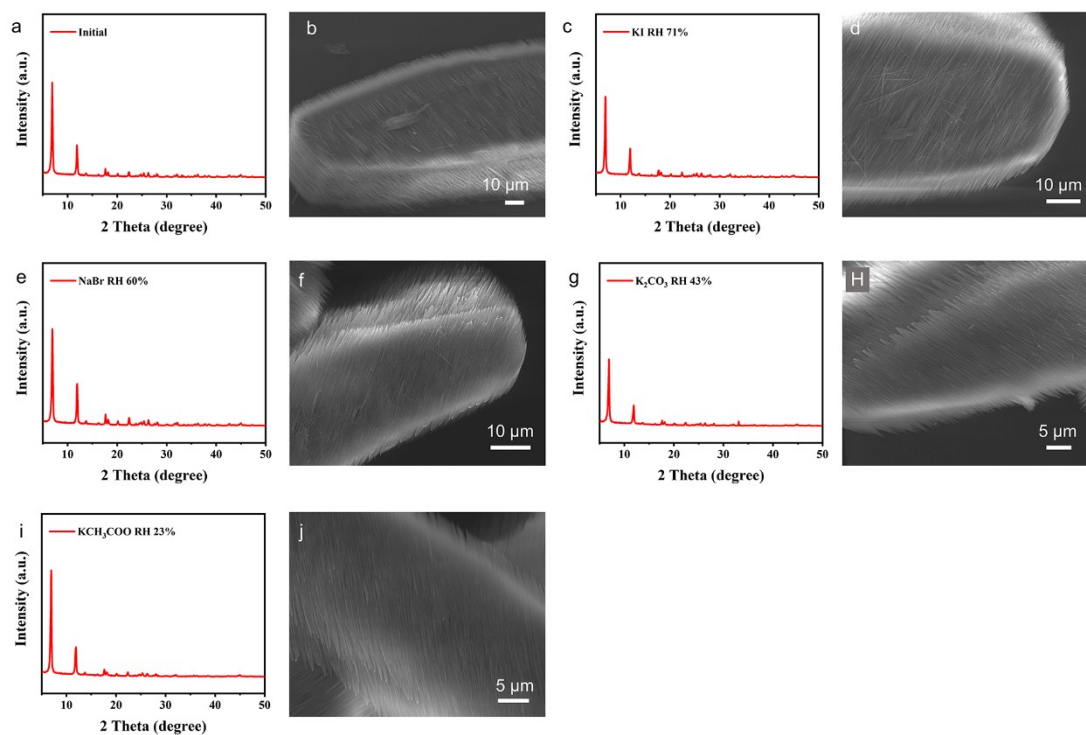


**Fig. S9** The XPD patterns and SEM images of (a-b) initial OMS sample before the stability test, (c-d) the OMS sample kept in the container with saturated KI solution (RH 71%), (e-f) the OMS sample kept in the container with saturated NaBr solution (RH 60%), (g-h) the OMS sample kept in the container with saturated  $K_2CO_3$  solution (RH 43%), and (i-j) the OMS sample kept in the container with saturated  $KCH_3COO$  solution (RH 23%).

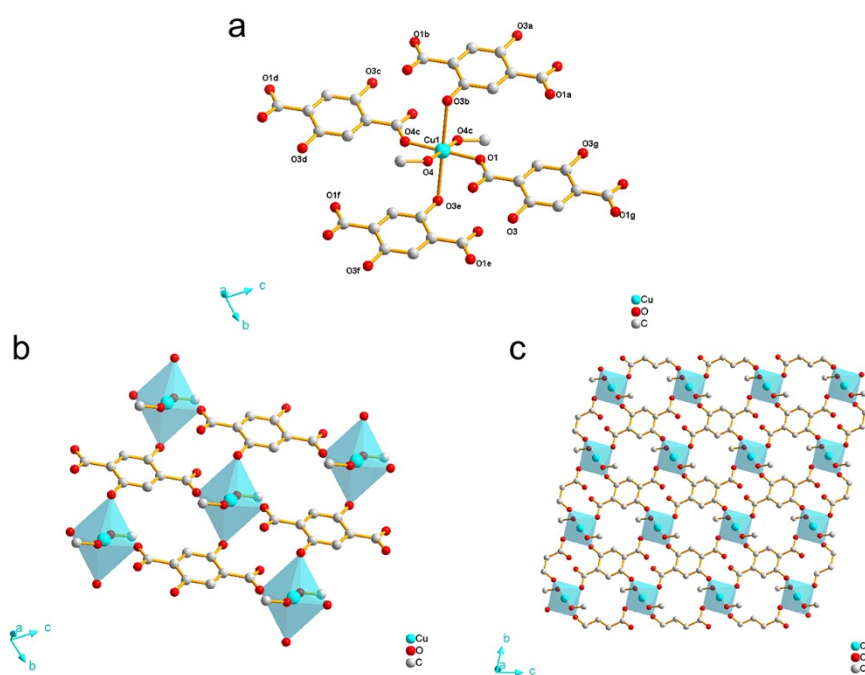


**Fig. S10** Crystal structure of PMC-m. (a) The fundamental unit of PMC-m. (b) The coordination environment of Cu<sup>2+</sup> in PMC-m. (c) The 2D layer structure of PMC-m. The hydrogen atoms are omitted for clarity. Symmetry codes: a) 1-x, -y, 2-z; b) x, -1+y, z; c) 1-x, -y, 1-z; d) x, -1+y, -1+z; e) 1-x, 1-y, 1-z; f) x, y, -1+z; g) 1-x, 1-y, 2-z.

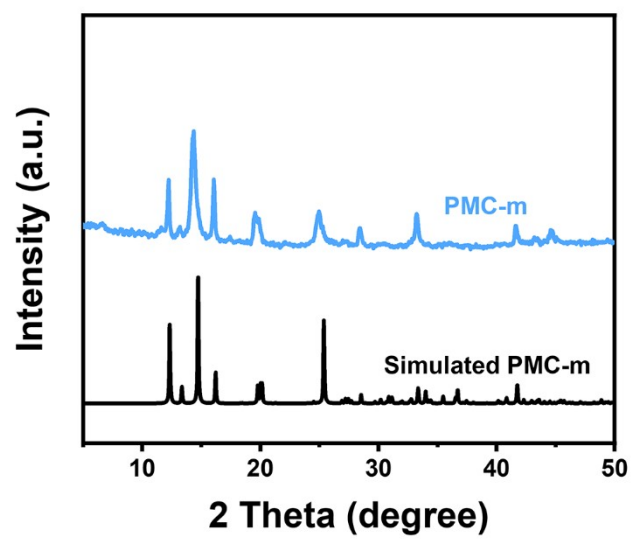


**Fig. S11** Simulated and measured PXRD pattern of PMC-m.

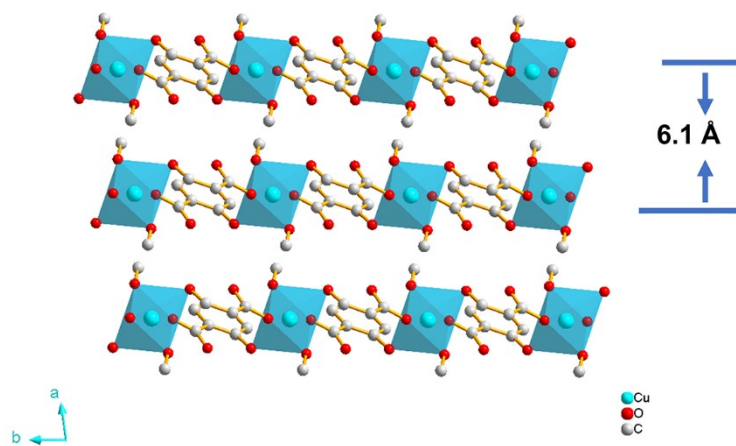


**Fig. S12** The stacked 2D-layer structures of PMC-m.

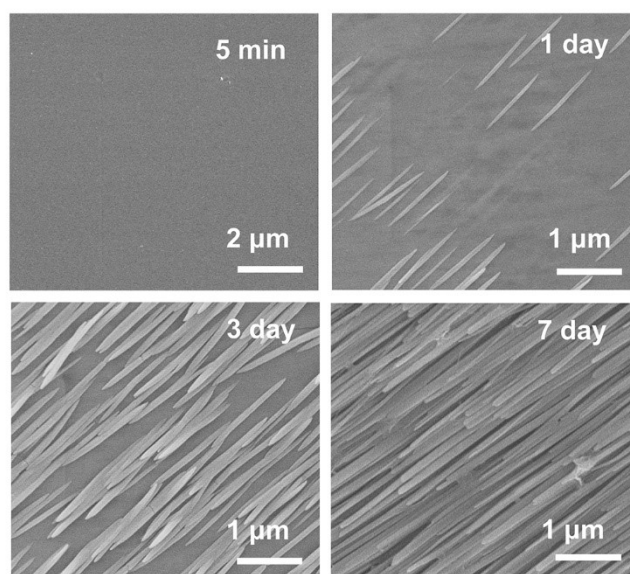


**Fig. S13** SEM images obtained during transformation of the crystals at different times.



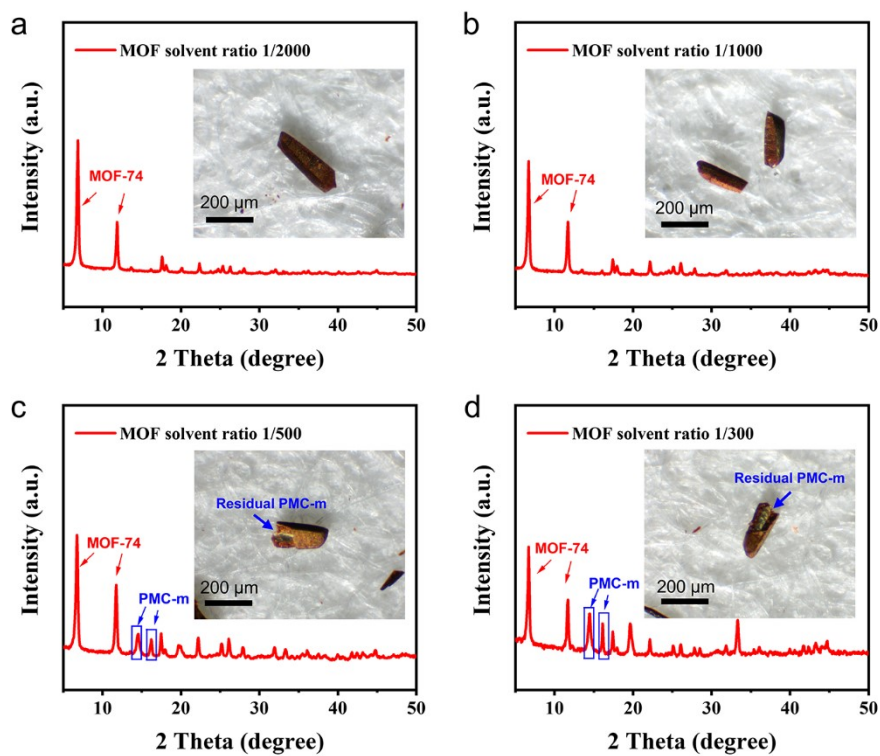


**Fig. S14** The XRD patterns and corresponding photographs of the obtained OMS sample after 2 weeks transformation with the MOF-to-solvent ratio of (a) 1/2000, (b) 1/1000, (c) 1/500, and (d) 1/300.

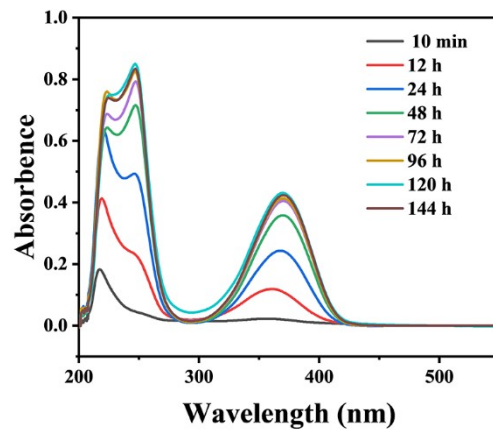


**Fig. S15** The UV-Vis absorption spectra of the methanol solution immersed with PMC crystals at different time points during the transformation process for PMC to OMS.

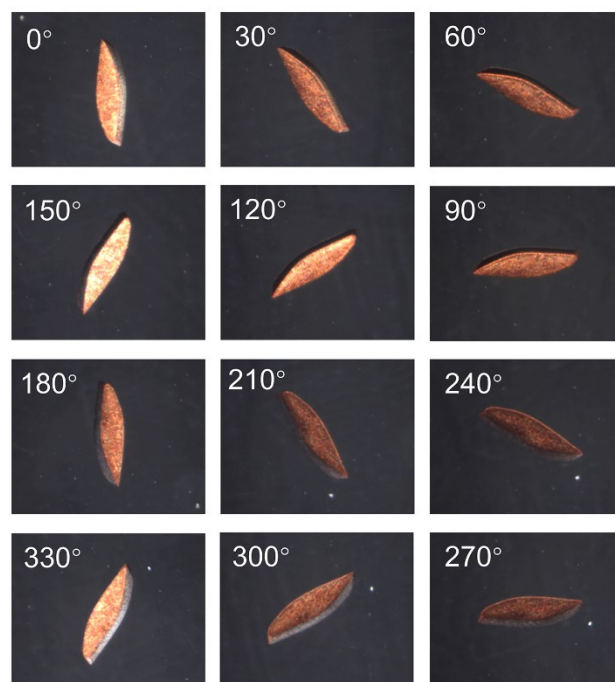


**Fig. S16** The optical photographs recorded with the CCD camera at different sample azimuth angle.

**Table S1** Crystal data and structure refinement for PMC.

Identification code	PMC	PMC-m
Empirical formula	C <sub>14</sub> H <sub>22</sub> CuN <sub>2</sub> O <sub>10</sub>	C <sub>10</sub> H <sub>12</sub> CuO <sub>8</sub>
Formula weight	441.87	323.74
Temperature	100(2) K	193.00 K
Wavelength	0.71073 Å	1.54178 Å
Crystal system	Triclinic	Triclinic
Space group	<i>P</i> -1	<i>P</i> -1
Unit cell dimensions	a = 6.9500(4) Å	a = 6.1190(6) Å
	b = 7.3157(4) Å	b = 6.8615(5) Å
	c = 9.1986(6) Å	7.3913(5) Å
	α = 91.164(2)°.	α = 77.070(5)°.
	β = 98.148(2)°.	β = 82.627(7)°.
	γ = 102.677(2)°.	γ = 80.507(7)°.
Volume	451.05(5) Å <sup>3</sup>	296.96(4)
Theta range for data collection	3.04 to 29.59°.	6.686 to 77.898
Goodness-of-fit on F <sup>2</sup>	1.071	1.101
Final R indices [I > 2σ(I)]	R1 = 0.0239, wR2 = 0.0649	R1 = 0.0833, wR2 = 0.2315
R indices (all data)	R1 = 0.0247, wR2 = 0.0656	R1 = 0.0962, wR2 = 0.2474
CCDC number	2088590	2206564

**Table S2** Assignment of absorption bands from FT-IR spectra of transformed OMS.

Group	OHN	Assignment
1	1573.2 cm <sup>-1</sup>	$\nu_{\text{as}}$ (COO <sup>-</sup> )
2	1497.5 cm <sup>-1</sup>	$\nu$ (CC)
2	1455.7 cm <sup>-1</sup>	$\nu$ (CC)
2	1371.3 cm <sup>-1</sup>	$\nu_{\text{s}}$ (COO <sup>-</sup> )
3	1243.4 cm <sup>-1</sup>	$\nu$ (C-O) phenolate
4	1192.7 cm <sup>-1</sup>	$\beta$ (C-H)
4	1122.9 cm <sup>-1</sup>	$\beta$ (C-H)

**Table S3** The frequently used kinetic mechanisms model.

Model	Integral form $g(\alpha) = kt$
Nucleation models:	
Power law (P2)	$\alpha^{1/2}$
Power law (P3)	$\alpha^{1/3}$
Power law (P4)	$\alpha^{1/4}$
Avrami-Erofeev (An)	$[-\ln(1 - \alpha)]^{1/n}$ (n: Avrami exponent)
Avrami-Erofeev (A2)	$[-\ln(1 - \alpha)]^{1/2}$
Avrami-Erofeev (A3)	$[-\ln(1 - \alpha)]^{1/3}$
Avrami-Erofeev (A4)	$[-\ln(1 - \alpha)]^{1/4}$
Geometrical contraction models:	
Contracting area (R2)	$1 - (1 - \alpha)^{1/2}$
Contracting volume (R3)	$1 - (1 - \alpha)^{1/3}$
Diffusion models:	
1-D diffusion (D1)	$\alpha^2$
2-D diffusion (D2)	$((1 - \alpha)\ln(1 - \alpha)) + \alpha$
3-D diffusion–Jander (D3)	$(1 - (1 - \alpha)^{1/3})^2$
Ginstling–Brounshtein (D4)	$1 - (2/3)\alpha - (1 - \alpha)^{2/3}$
Reaction-order models:	
Zero-order (F0/R1)	$\alpha$
First-order (F1)	$-\ln(1 - \alpha)$
Second-order (F2)	$[1/(1 - \alpha)] - 1$
Third-order (F3)	$(1/2)[(1 - \alpha)^{-2} - 1]$